### 2.3.5.1.3. *Source intensity distribution and size*

The intensity distribution of the focal line is usually not uniform. This has no apparent effect on the shapes of powder reflections but may cause difficulties with single crystals (Parrish, Mack & Taylor, 1966). The distribution can be measured with a small pinhole placed between the X-ray tube focal line and a dental or Polaroid film. The ratio of the distances between line-to-pinhole and pinhole-to-film determines the magnification of the image. The pinhole diameter should be small for good resolution. About 0.1 mm diameter is satisfactory and can be made with a special microdrill, spark erosion or other methods. The thickness of the metal must be minimal to avoid having the aperture formed by the length and diameter of the pinhole limit the length of focus photographed. Avoid over-exposure which broadens the image. Also, the Polaroid film should be exposed outside the cassette to avoid broadening caused by the intensifying screen.

A more accurate method is to scan a slit and detector (mounted on the same arm) normal to the central ray from the focus as shown in Fig. 2.3.5.2(*b*) (Parrish, 1967). The slits are a pair of molybdenum rods (or other high-absorbing metal) with opening normal to the scan direction, and the slit width determines the resolution. This method gives a direct measurement of the intensity distribution from which the projected size can be determined.

The actual size of the focus $F'_w$ is foreshortened to $F_w$ by the small take-off angle $\psi$, $F_w = F'_w \sin\psi$. A typical $0.5 \times 10$ mm focus viewed at 6° appears to be a line $0.05 \times 10$ mm or a spot $0.05 \times 1$ mm [Fig. 2.3.1.9(*a*)]. The line focus is generally used for powder diffractometry and focusing cameras and the spot focus for powder cameras and single-crystal diffractometry.

X-rays emerge from three or four Be windows spaced 90° apart around the circumference. Their diameter and position with respect to the plane of the target determine the usable $\psi$-angle range. The length of line focus that can pass through the window can be seen with a flat fluorescent screen in the specimen holder using the largest entrance slit. The Be window thickness often used is 300 µm and the transmission as a function of wavelength is shown in Fig. 2.3.5.2(*a*).

### 2.3.5.1.4. *Air and window transmission*

The absorption of X-rays in air is also wavelength-dependent and increases rapidly with increasing wavelength, Fig. 2.3.5.2(*a*). The air absorption was calculated using a density

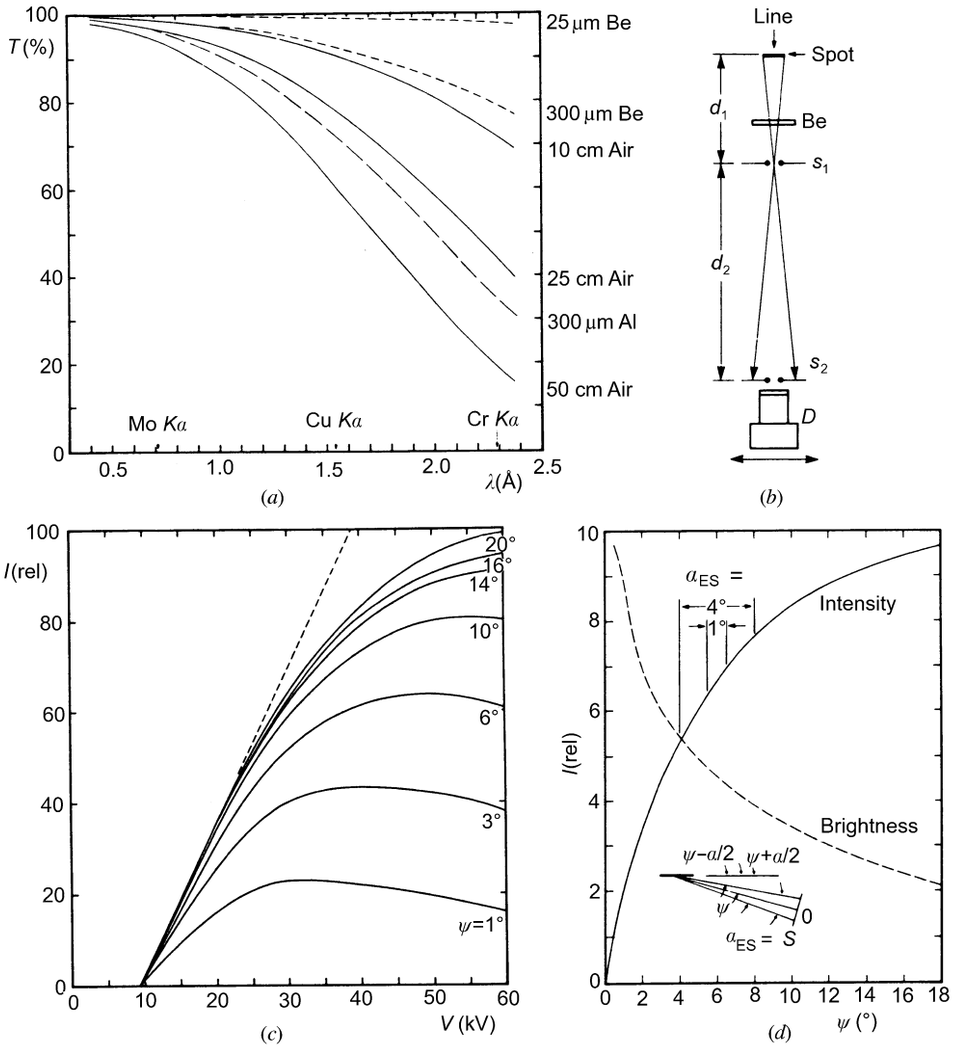


Fig. 2.3.5.2. (*a*) Transmission of Be, Al and air as a function of wavelegth. (*b*) Method for measuring X-ray tube focus by scanning slit $S_2$ and detector $D$. Slit $S_1$ is fixed and the radio of the distances $d_2/d_1$ gives the magnification. (*c*) Intensity of a copper target tube as a function of kV for various take-off angles. (*d*) Intensity and brightness as a function of take-off angle of a copper target tube operated at 50 kV. The intensity distributions for 1 and 4° entrance-slit apertures are shown at the top, and terms used to define $\psi$ and $\alpha_{ES}$ are shown in the lower insert.

of 0.001 205 g cm$^{-3}$ at 760 mm Hg pressure (1 mm Hg = 133 Pa), 293 K, and 0% humidity. Changes in the humidity and barometric pressure can cause small changes in the intensity. Baker, George, Bellamy & Causer (1968) measured the intensity of the Cu $K\alpha$ and barometric pressure over a 5 d period and found the counts increased 2.67% as the barometric pressure decreased 3.7%. However, they used an Xe proportional counter whose sensitivity is also pressure-dependent and a large amount of the change may have been due to changes in the detector efficiency.

Air scattering increases rapidly at small $2\theta$'s, increasing the background. It is advisable to use a vacuum or helium path to avoid problems in this region.

#### 2.3.5.1.5. *Intensity variation with take-off angle*

The intensity of the characteristic line spectrum emerging from the tube depends on the anode element, voltage, and take-off angle $\psi$. The depth of penetration of the electrons in the anode is approximately proportional to $kV^2/\rho$, where $\rho$ is the density of the anode metal. The path length $L$ of the X-rays to reach the surface depends on the depth $D$ at which they are generated and the take-off angle, $L = D/\sin\psi$. Self-absorption in the anode causes a loss of intensity that increases with $D$ and decreasing $\psi$. The intensity of Cu $K\alpha$ radiation at 50 kV as a function of take-off angle is shown in Fig. 2.3.5.2(*d*). This effect has been described in a number of publications: Green (1964), Brown & Ogilvie (1964), Birks, Seebold, Grant & Grosso (1965), Parrish (1968), and Phillips (1985). Because of the self-absorption, the wavelength distribution varies slightly with take-off angle (Wilson, 1963, pp. 61–63).

The optimum kV and mA operating conditions are not sharply defined and the range can be determined with a powder reflection or by using small apertures in the direct beam with balanced filters and pulse-amplitude discrimination. The intensity is measured at various voltages, keeping the current constant and converting the data to constant power. Typical experimental curves relating Cu $K\alpha$ intensity to kV for various $\psi$'s are given in Fig. 2.3.5.2(*c*). At 50 kV, the intensity doubles by increasing $\psi$ from 3 to 12° (although the projected width of the focal spot also increases). The effect is much larger for Cr $K\alpha$ and W $L\alpha$ because of their higher absorptions. The linear region of *I versus V* is relatively short and increases with $\psi$. At small $\psi$'s, $I$ is virtually independent of $V$ and could decrease with increasing voltages; increasing the current would give a greater increase using the same power. For a tube with maximum power values of 60 kV, 55 mA and 2200 W, the relative intensites of Cu $K\alpha$ are about 100 for 40 kV/55 mA, 88 for 50 kV/44 mA and 74 for 60 kV/37 mA. However, the filament life decreases with increasing current and most manufacturers specify a maximum allowable current.

The intensity distribution reaching the specimen is not uniform over the entire illuminated area. In the direction normal to the specimen axis of rotation, one end of the specimen views the X-ray tube focus at an angle $\psi - (\alpha/2)$ and the other at $\psi + (\alpha/2)$, where $\alpha$ is the angular aperture of the entrance slit [Fig. 2.3.5.2(*d*)]. The intensity differences are determined by $\psi$ and $\alpha_{ES}$ so that the centre of gravity does not coincide with the geometrical centre. The dependence of the diffracted-beam intensity on the aperture of the entrance slit $\alpha_{ES}$, therefore, may also be nonlinear. For example, at $\psi = 6°$, the intensity difference at the ends of the specimen is 9% for $\alpha_{ES} = 1°$, and 44% for $\alpha_{ES} = 4°$; the corresponding numbers for $\psi = 12°$ are 2 and 10% respectively.

Although increasing $\psi$ increases the intensity, it also increases the projected width and may increase the widths of the reflections (§2.3.1.1.5). The brightness expressed as $I(\text{rel})/\sin\psi$ also decreases rapidly. When one is working with small apertures, as in grazing incidence and the analysis of small samples, the brightness becomes a very important factor in obtaining the maximum number of counts. For example, the intensity at $\psi = 12°$ is twice that at 3° but the brightness is one half [Fig. 2.3.5.2(*d*)]. However, it should be noted that the smaller the take-off angle the greater the possibility of intensity losses due to target roughening.

### 2.3.5.2. *X-ray spectra*

The X-ray tube spectrum consists of sharp characteristic lines superposed on broad continuous radiation as shown in Fig. 2.3.5.3. The continuous spectrum begins at a wavelength determined by the voltage on the X-ray tube, $\lambda\,\text{min} \simeq 12.4/\text{kV}$. It reaches a maximum at about 1.5 to $2\lambda\,\text{min}$ and gradually falls off with increasing $\lambda$ [Fig. 2.3.5.4(*a*)]. The intensity increases with voltage and current, and also with the atomic number of the target element. The integrated intensity is greater than that of the spectral lines. It is used for Laue patterns, fluorescence analysis, and energy-dispersive diffraction. It is troublesome in powder diffraction because it contributes to the background by scattering and by causing specimen fluorescence.

The wavelengths of the spectral lines decrease with increasing atomic number $Z$ of the target element [Moseley's law, Fig. 2.3.5.4(*b*)]. All the lines in a series appear when the critical excitation voltage is exceeded. For a Cu target, this is 9 kV and the approximate relative intensities are Cu $K\alpha_2$ 50, $K\alpha_1$ 100 and $K\beta$ 20. The peak intensities of Cu $K\alpha_1$ and Cu $K\alpha_2$ in diffractometer patterns may not be exactly 2:1 but closer to 2.1:1 in resolved doublets because of the different profile widths. The profile widths of the spectral lines vary among the different elements used for X-ray tube targets (Compton & Allison, 1935), as does the $K\beta/K\alpha$ ratio (Smith, Reed & Ware, 1974). The observed ratio varies with the degree of overlap. The rate of increase with voltage and other factors is described above.

A broad weak group of satellite peaks, $K\alpha_3$, occurs near the bottom of the short-wavelength tail of the $K\alpha_1$ peak (see Fig. 2.3.3.3). The intensity varies with the target element and is about 0.5% for the Cu $K$ spectrum. The satellites appear as a small, broad, ill defined peak in powder diffraction patterns (Parratt, 1936; Parrish, Mack & Taylor, 1963; Edwards & Langford, 1971).

The spectral lines have an approximately Lorentzian shape when measured with a two-crystal diffractometer. They usually have a small asymmetry and their widths vary among the elements and also in the same series of lines. Bearden (1964) defined the wavelength as the peak determined by extrapolation of the centres of chords near the top of the peak. The corresponding energy levels have been compiled by Bearden & Burr (1965). The centroid of the $K\alpha_1$, $K\alpha_2$ peaks of Cu and Fe has been calculated from the Bearden experimental two-crystal data (Mack, Parrish & Taylor, 1964). X-ray wavelengths are discussed in Chapter 4.2. The standard targets provide the $K$ spectra of Ag, Mo, Cu, Co, Fe and Cr, and the W $L$ spectrum. Other targets may be obtained on special order. The $K$ spectra of the elements of high atomic number require a radiographic tube and power supply that can operate continuously at about 150 kV or higher. (**Caution:** The radiation-shielding problems multiply exponentially at high voltages.)